Microchimica Acta
https://doi.org/10.1007/s00604-019-3252-9

ORIGINAL PAPER

Molecular beacon immobilized on graphene oxide for enzyme-free signal amplification in electrochemiluminescent determination of microRNA

Jiaxing Wang[1] · Linlin Zhang[1] · Liping Lu[1] · Tianfang Kang[1]

Received: 25 September 2018 / Accepted: 13 January 2019

Abstract

An electrochemiluminescence (ECL) based biosensor is described for determination of microRNAs in the A549 cell line. Firstly, graphene oxide (GO) is dripped onto a glassy carbon electrode surface to form an interface to which one end of the capture probe (with a stem-loop structure) can be anchored through π-interaction via dangling unpaired bases. The other end of the capture probe is directed away from the GO surface to make it stand upright. Target microRNAs can open the hairpin structure to form a double-stranded DNA-RNA structure. Two auxiliary probes, generating a hybridization chain reaction, are used to elongate the DNA duplex. Finally, doxorubicin-modified cadmium telluride quantum dot nanoparticles (Dox-CdTe QD) are intercalated into the base pairs of the hybrid duplexes to act as signalling molecules. The ECL signal of the Dox-CdTe QD increases proportionally with the concentration of microRNAs, specifically for microRNA-21. The assay covers a wide linear range (1 fM to 0.1 nM), has a low detection limit for microRNA-21 (1 fM), and is selective, reproducible, and stable.

Keywords CdTe · Doxorubicin · π-stacking interaction · DNA probe · Hybridization chain reaction

Introduction

Thousands of microRNAs have been identified that act as promising biomarkers for early screening, clinical staging, diagnosis, and the prediction of human diseases [1, 2]. Therefore, researchers have been devoted to microRNA detection sensitively. However, the intrinsic properties of MicroRNAs, such as instability, short sequence lengths, low abundance, and sequence similarity among family members [3], hinder progress in the development of detection techniques. Northern blotting [4], real-time PCR [5], and microarray analysis [6], the conventional methods for MicroRNAs detection, suffer from low sensitivity, harsh experimental conditions, time-consuming procedures, and expensive equipment, which restrict their practical application.

Various signal readout methods for the detection of microRNAs have been developed based on electrochemical biosensors [7], fluorescence [8], and surface plasmon resonance [9]. To enhance the sensitivity, improve the selectivity, and lower the detection limit and cost, people are paying more and more attention to the electrode surface modified materials [10–13]. Therefore, various modified electrodes using nanomaterials and precious metals have emerged [14, 15], which also provides more possibilities for fixing probes on the electrode surface. Immobilization of the DNA probe is also a key step for DNA sensor fabrication because it usually improves the stability of the DNA and ensures successful hybridization of the probe DNA with the target MicroRNAs. Furthermore, the detection limits of biosensors can be greatly reduced by increasing the extent of DNA immobilization and the control over the molecular orientation of probe DNA. Therefore, developments in DNA biosensor fabrication have focused on new support materials for effective immobilization of DNA, and many new functional materials, such as polymers, ionic liquids, and nanoparticles, have been exploited [16–18].

Electronic supplementary material The online version of this article (https://doi.org/10.1007/s00604-019-3252-9) contains supplementary material, which is available to authorized users.

✉ Liping Lu
lipinglu@bjut.edu.cn

[1] Key Laboratory of Beijing on Regional Air Pollution Control, Beijing University of Technology, Beijing 100124, China

Published online: 01 February 2019

Graphene oxide (GO), a single-atom-thick, 2-dimensional carbon nanomaterial [19], has attracted great interest in the biosensor field because of its favorable physical and chemical properties [20]. GO can bind single-stranded DNA (ssDNA) through the π-stacking interaction between the rings of the nucleobases and the hexagonal cells of the graphene [21]. However, when a complementary strand is added, the resulting dsDNA rapidly detaches from the GO surface because of its poor affinity to GO [22].

In this work, we desribe a sensitive biosensor for microRNAs using GO as a base material. The GO binds to hairpin DNA, one end of which is a single chain with six cytosine bases, to achieve double-stranded partial standing. The use of GO simplifies the immobilization process by obviating the need for a linker, resulting in lower cost. In this sensing system, two specially designed auxiliary hairpin DNA probes (denoted H_1 and H_2) are employed to induce hybridization chain reaction (HCR). Doxorubicin-combined quantum-dot (Dox-QD) nanoconjugates, intercalated into the dsDNA hybrids, are used as the signal detector. Doxorubicin is an anthracycline that can be inserted into DNA base pairs [23, 24]. And the quantum dots react readily with doxorubicin to form a N-acetyl-L cysteine/cadmium telluride-quantum dots/doxorubicin complex via electrostatic attraction between the - NH_3^+ moiety of doxorubicin and the - COO^- moiety of N acetyl-L-cysteine/cadmium telluride quantum dots [25]. So, a signal amplification label (doxorubicin-combined quantum-dot nanoconjugates) can intercalate into the base pairs of the hybrid duplex structures with its functional Dox groups and act as ECL emitters. The sensor achieves better sensitivity and selectivity than some previous methods of microRNA detection.

Experimental

Materials and reagents

N-Acetyl-L-cysteine (NAC), *N*-(3-dimethylaminopropyl)-*N*′-ethylcarbodiimide hydrochloride (EDC), and bovine serum albumin (BSA) were purchased from Sigma-Aldrich Chemical Co. (St. Louis, USA, https://www.sigmaaldrich.com). Sodium tellurite (Na_2TeO_3) and doxorubicin (Dox) were from Aladdin industrial corporation (Shanghai, China, http://www.aladdin-e.com). $NaBH_4$, $Na_2HPO_4{\cdot}12H_2O$, $NaH_2PO_4{\cdot}2H_2O$, $CdCl_2$, C_2H_5OH, NaOH, and $K_2S_2O_8$ were received from Tian Jin Fu Chen Chemical Reagents Factory (Tianjin, China, http://www.tjfch.com). GO (0.5 mg mL^{-1}) was purchased from Nanjing Xian Feng Nano Co. (Nanjing, China, https://www.xfnano.com). All the chemicals used were of analytical grade and all solutions were prepared with ultrapure water obtained from a Milli-Q water purification system (Millipore Corp., Bedford, MA, http://www.millipore.com).

Synthetic DNA was ordered from Sangon Biological Co., Ltd. (Shanghai, China, https://www.sangon.com). MicroRNAs, diethylpyrocarbonate (DEPC), and Dulbecco's Modified Eagle Medium (DMEM) were ordered from Gene Pharma (Shanghai, China, http://www.genepharma.com). A 5 mM solution of phosphate-buffered saline (PBS, pH 7.4) was used as the DNA immobilization buffer and washing buffer. RNAs were dissolved in DEPC. All experiments involving microRNAs were carried out without RNase. All centrifuge tubes, test tubes and beakers were sterile and enzyme-free. The sequences of the oligonucleotides are listed in Table 1.

Apparatus

Electrochemical measurements were performed on a CHI 660D electrochemistry workstation (CH Instruments Inc., Shanghai, China, http://www.chinstr.com). A conventional three-electrode configuration was used, with a modified glassy carbon electrode (GCE, 3 mm in diameter), a Ag/AgCl (3 M KCl) reference electrode, and a platinum wire counter electrode. The ECL emission was monitored by an MPI-A electrochemiluminescence analyzer (Xi'an Remax Electronic Science & Technology Co. Ltd., Xi'an, China, http://remax.testmart.cn) in 0.1 M PBS (saline; pH 7.4) containing 0.1 M KCl and 0.1 M $K_2S_2O_8$ with the voltage of the photomultiplier tube (PMT) at 600 V. A magnetic stirrer was obtained from Jintan Hongyuan Instrument Factory, China. A KQ218 ultrasonic cleaner was obtained from Kunshan Ultrasonic Instrument Co., Ltd., China. http://www.ks-csyq.com. Centrifugation was performed using a Centrifuge 5424 from Eppendorf Ltd., Germany. https://www.eppendorf.com.

Pretreatment of the probes

Three species of DNA hairpin probes, which were rationally designed according to the DNAMAN (Highly integrated molecular biology comprehensive application software, https://www.lynnon.com/dnaman.html), are listed in Table 1. Before use, the hairpin probes were incubated at 95 °C for 5 min and then slowly cooled to room temperature (2 °C min^{-1}) in 1 × PBS buffer to ensure the probes were perfectly folded into a hairpin structure.

Assembly of the DNA biosensor for detecting microRNA-21

A schematic representation of the stepwise fabrication procedure for the proposed biosensor is shown in Scheme 1. At the beginning of assembly, the GCE was polished with 0.05 μm alumina powder on a microcloth pad and rinsed thoroughly with ultrapure water. Then the polished electrode was washed successively with ultrapure water, anhydrous ethanol, and

Table 1 Oligonucleotide sequences used in this study

Capture DNA	5`-CCCCCCTCAACATCAGTCTGATAAGCTAGAGATGTTAT-3`
microRNA-21	5`-UAGCUUAUCAGACUGAUGUUGA −3`
H_1-DNA (H_1)	5`- TGTTATGGAAATAACATCTC -3`
H_2-DNA (H_2)	5`- TTCCATAACAGAGATGTTAT −3`
Single-base mismatch microRNA	5`-UAGCUUAUCGGACUGAUGUUGA −3`
Three-base mismatch micoRNA	5`-UUGCUUAUCGGACUGAUCUUGA −3`
microRNA-205	5`-UCCUUCAUUCCACCGGAGUCUGU -3`

ultrapure water in an ultrasonic bath. After the electrode was dried by nitrogen blowing, 5 μL of graphene oxide (0.1 mg mL^{-1}) was dripped onto the electrode surface and dried at room temperature (labeled GO/GCE). After washing the electrode surface with ultrapure water, 5 μL buffer containing 12 μM capture probes was dripped onto the electrode surface, which was then kept for 60 min at 37 °C (labeled DNA/GO/GCE). The electrode was then thoroughly rinsed with 5 mM PBS (saline) and ultrapure water, and incubated in 1 mg mL^{-1} BSA solution for 45 min to avert nonspecific DNA adsorption on the GO surface. After thorough rinsing, 5 μL aliquots of solutions containing the target microRNA at various concentrations were placed on the modified electrode to incubate for 60 min. Then the electrode was rinsed and dried. Finally, 10 μL of a freshly prepared buffer containing 1 μM auxiliary probe H_1 and 1 μM auxiliary probe H_2 was dripped onto the surface of the electrode, and incubated for 120 min at 37 °C to self-assemble into DNA concatamers. After that, a 5 μL droplet of Dox-QD nanoconjugates (see ESM) was cast onto the modified electrode and incubated for 8 h. These steps were carried out in a wet box.

Finally, after washing with 5 mM PBS (saline), the resulting functionalized electrode was placed in detection buffer (0.1 M PBS containing 0.1 M $K_2S_2O_8$, pH 7.4) for ECL measurement. The measurements were performed with potential scanning from 0 to −1.5 V (versus Ag/AgCl) at the scan rate of 0.1 V s^{-1} with the voltage of the PMT at 600 V.

Cell culture and total RNA extraction

All appliances were pretreated with 0.01% DEPC solution, and the solutions used throughout the experiments were prepared with DEPC-treated water. The human cancerous cell lines (A549) were cultured in DMEM containing 4.5 g L^{-1} of D-glucose and supplemented with 10% fetal bovine serum at 37 °C with 5% CO_2.

Total microRNA samples were extracted from each cell line using Trizol Reagent (Invitrogen Biotechnology Co., Ltd.) according to the manufacturer's protocol. Briefly, the appropriate amount of Trizol Reagent was added to the cell pellet for cell disruption, followed by incubation at room temperature for 5 min. Subsequently, the microRNA extraction was precipitated by 2-propanol. Finally, the extracted microRNA solution was diluted by DEPC and stored at −20 °C for further use.

Results and discussion

Feasibility and electrochemical characterization of sensor

The signal amplification capability of our sensor was confirmed by comparing the analytical signal intensity of with or without apply HCR method when target RNA was incubated. As shown in Fig. 1a, curve b indicates the signal intensity

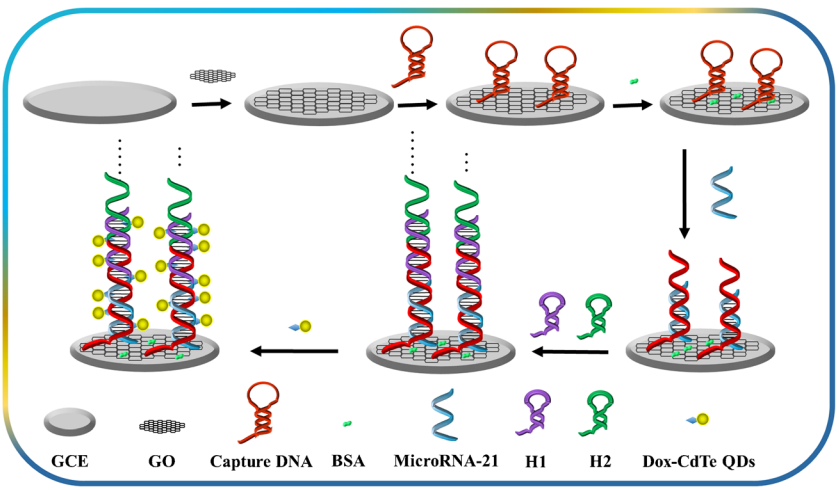

Scheme 1 Schematic representation of the stepwise ECL biosensor fabrication process

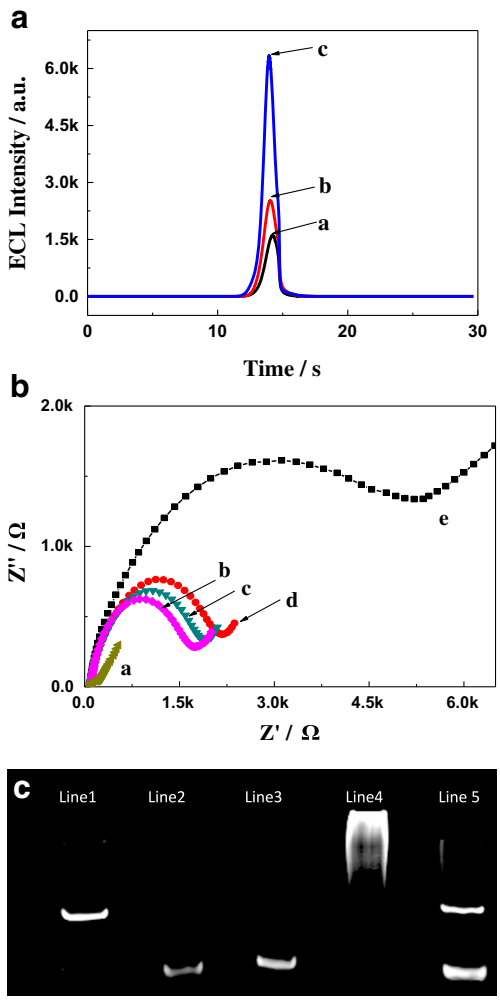

Fig. 1 **a** ECL intensity curves incubated with Dox-QD of (**a**) DNA/GO/GCE, (**b**) RNA-DNA/GO/GCE, (**c**) H1-H2/RNA-RNA/GO/GCE. ECL curves were recorded in PBS containing 0.1 M $K_2S_2O_8$ from 0 to 1.5 V. **b** Electrochemical impedance spectra of the electrode at different stages of modification in the presence of 0.1 M KCl containing a 5 mM $K_4[Fe(CN_6)]/K_3[Fe(CN_6)]$ mixture: (**a**) bare GCE, (**b**) GO/GCE, (**c**) DNA/GO/GCE, (**d**) RNA/DNA/GO/GCE, (**e**) H_1-H_2/ RNA/DNA/GO/GCE. **c** The PAGE images for DNA and HCR product: lane 1, capture DNA; lane 2, H_1-DNA; lane 3, H_1-DNA; lane 4, the HCR product with the target microRNA (capture DNA, microRNA-21, H_1 and H_2); lane 5, the reaction without the target microRNA (capture DNA, H_1 and H_2)

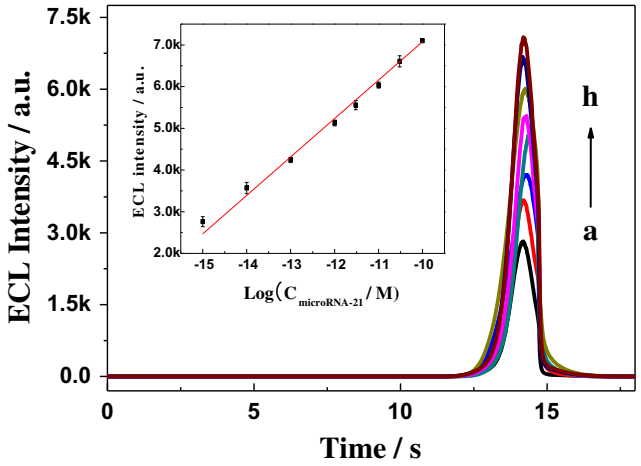

Fig. 2 ECL responses of the sensor to different concentration of microRNA-21: (**a**) 1 fM, (**b**) 10 fM, (**c**) 100 fM, (**d**) 1 pM, (**e**) 3 pM, (**f**) 10 pM, (**g**) 30 pM, and (**h**) 100 pM. Inset: The resulting calibration plot of log $C_{microRNA-21}$ vs ECL intensity, where $C_{microRNA-21}$ is the concentration of target RNA. The error bars represent the standard deviation of three repeat measurements

of without apply HCR method, while curve c corresponds to the signal intensity of the proposed HCR assay which is constructed with two hairpin DNA. In addition, curve a is the background signal when the target RNA is not present. As expected, curve c exhibits a considerable increase in ECL intensity compared with curve b, suggesting the noticeable signal amplification effect of our HCR-based protocol. This is because a single target DNA hybridizes with only one single capture probe to form a partial dsDNA, which limits the total signal gain from the intercalated Dox-QD and thus shows poor sensitivity. In contrast, a long dsDNA polymer structure is formed in the HCR assay and enables numerous Dox-QD to be intercalated into the DNA, resulting in ECL intensity enhanced obviously.

The surface features of the modified electrodes were examined using electrochemical impedance spectroscopy (EIS). The EIS spectra of the modified GCE electrode were measured at each modification step, and the results are illustrated as a Nyquist plot in Fig. 1b. This plot takes the shape of a semicircle in the high-frequency region but a straight line in the low-frequency region, demonstrating that the electrolysis process was controlled by electron transfer at high frequency and by diffusion at low frequency [26]. The EIS measurements were performed in 0.1 M KCl containing 5 mM $K_4[Fe(CN_6)]/K_3[Fe(CN_6)]$. Fig. 1b shows the EIS results at the different steps of electrode modification. In these impedance spectra, an increase in the semicircle diameter indicates an increase in the electron transfer resistance (R_{et}) at the interface [27]. It can be seen that the bare electrode exhibited only a tiny semicircle domain, which implies fast electron transfer. When GO was self-assembled onto the electrode, R_{et} increased compared with the bare electrode. This indicates that GO effectively blocked the underlying electron transfer of the supporting electrode substrate, likely because of its large basal and low edge-plane content and the repulsive interaction of $[Fe(CN_6)]^{3-/4-}$ with negatively charged of GO [28, 29]. When the capture probe was self-assembled onto the modified electrode, the impedance increased further. This is attributed to the negative charges on the phosphate backbone of the self-assembled capture probe DNA, which electrostatically repelled the $Fe(CN)_6^{4-/3-}$ anions. The value of R_{et} further increased upon the incubation of BSA and the target microRNA on the electrode. After the formation of a long DNA chain promoted by the auxiliary probes, R_{et} was further dramatically enlarged. The results of EIS confirmed the

Table 2 Analytical performance comparison of the described strategy with the selected previously published methods for microRNA detection

Materials or Reagent	Methods	Linear range	Detection limit	Reference
Multi-walled carbon nanotubes/Methylene blue	DPV	0.1 pM to 0.5 nM	84.3 fM	[30]
Thiolated probe-functionalized gold nanorods/GO/Oracet blue	DPV	2 fM to 8 pM	0.6 fM	[31]
Nafion-carbon nanotubes /Polyvinylpyrrolidone/AuNP	ECL	40 fM to 1 pM	20 fM	[32]
AuNP/Boron doped graphene quantum dots	ECL	100 fM to 10 nM	100 fM	[33]
DNA polymerase/Poly(thymine) strand/CuNPs	Fluorescence	70 fM to 700 nM	0.27 fM	[34]
Poly T- CuNPs/Duplex-specific nuclease/Terminal deoxynucleotidyl transferase	Fluorescence	20 pM to 1 nM	20 pM	[35]
GO/Dox-QD/H_1 and H_2 auxiliary probes	ECL	1 fM to 0.1 nM	1 fM	This work

successful capture of the target microRNA-21 and the formation of long DNA concatamers. Beside, polyacrylamide gel electrophoresis (PAGE) image proved microRNA's ability to open this hair-pin DNA construct and was shown in Fig. 1c. The mobility of a charged species in electrophoresis depends on its charge and molecular weight. The results showed lane 4 lagged behind lane 5, which indicated microRNA opened the hair-pin DNA and initiate the hybridization chain reaction. Lane 5 has no microRNA, which only appeared bands of probe, H_1 and H_2. It further proved that hair-pin DNA can not be opened if microRNA did not exit. These results were strong evidence that the HCR reaction and the electrode were fabricated as expected.

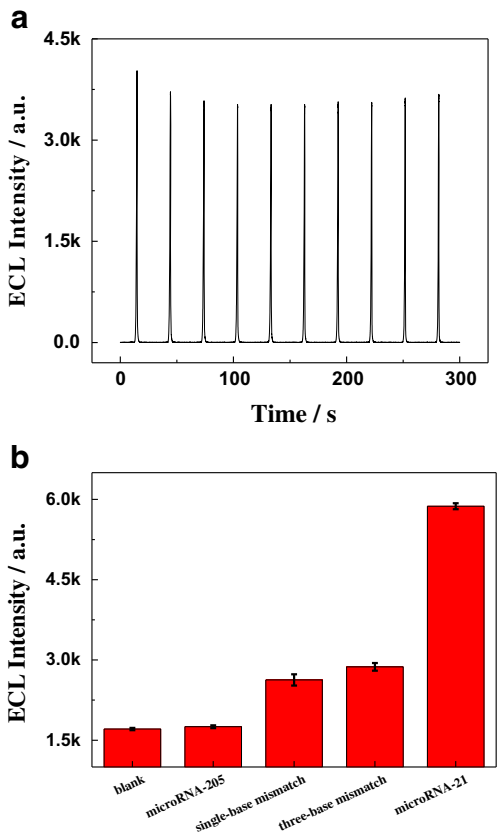

Fig. 3 **a** The ECL stability of the proposed biosensor incubated with 0.1 pM microRNA-21 using continuous cyclic potential scanning for 10 cycles. **b** Comparison of ECL responses to blank solution (0 M target microRNA-21), 10^{-11} M microRNA-205, single-base mismatch-microRNA, three base mismatch-microRNA, and 10^{-12} M target microRNA-21

Optimization of analytical conditions

The following parameters were optimized: (a) reaction time; (b) concentration of capture DNA; (c) optimal concentrations of H1 and H2. Respective data and Figures are given in the Electronic Supporting Material. The following experimental conditions were found to give best results: (a) Optimal reaction time: 8 h; (b) Optimal concentration of capture DNA: 12 μM; (c) Optimal concentrations of H1 and H2: 1 μM.(Fig.S2).

ECL detection of target microRNA-21

On the basis of the optimized experimental conditions, the quantitative performance of the proposed sensor with Dox-QD as indicators for microRNA analysis was examined by incubating the biosensor with different target microRNA-21 concentrations and recording the corresponding ECL responses. Fig. 2 shows the relationship between the ECL intensity and the concentrations of microRNA-21. It is clear that increasing concentrations of the target microRNA-21 resulted in an increase of the ECL signals. A linear relationship

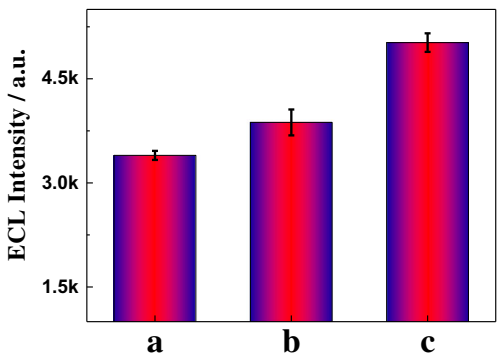

Fig. 4 ECL detection results of microRNA-21 in cell lysate samples from a human cancer cell line (A549) at different numbers: (**a**) 10^2 cells, (**b**) 5×10^2 cells, (**c**) 10^3 cells

between the ECL signals and the concentrations of microRNA-21 was obtained in the range from 1 fM to 0.1 nM, with a detection limit of 1 fM. The linear relationship can be represented as $y = 921.58\ x + 16{,}294.19$, with a correlation coefficient of $R^2 = 0.995$, where y is the ECL intensity and x is the concentration of microRNA-21. The obtained detection limit is relatively low, enabling highly sensitive detection across a wide concentration range. Hence, the biosensor shows promise for use in highly sensitive bioassays in clinical detection. And the analytical performance of this sensing system was compared with other electrochemical biosensing strategy for microRNA detection (Table 2).

Stability and selectivity of the ECL biosensor

The ECL stability of the proposed biosensor was explored by continuous cyclic potential scanning for 10 cycles at a microRNA-21 concentration of 0.1 pM. As is exhibited in Fig. 3a, the ECL intensity showed no obvious changes during cycling. This indicates the considerable stability of the newly developed biosensor. We attribute this favorable property to two causes. Firstly, the GO provided a good matrix for the loading of the DNA–RNA hybrids, thus increasing their accessibility to the probe. Secondly, the Dox-QD were more stable and highly active, leading to a remarkably amplified ECL signal output.

To investigate the specificity of the proposed method, three DNA sequences similar to the microRNA-21 target were selected as potentially interfering assay models, including one completely non-complementary microRNA (microRNA-205) and two base-mismatched RNA sequences. As revealed in Fig. 3b, the ECL intensity corresponding to the competing microRNA (microRNA-205) was essentially no different from that of the blank control experiment. The ECL responses in the presence of single-base mismatch microRNA and three-base mismatch microRNA showed only a slight increase compared with the blank test. Only the perfectly complementary microRNA-21 caused a substantial increase in signal intensity. These results indicated that the biosensor displayed good selectivity for the determination of microRNA-21.

Analysis of cell lysate samples

On the basis of the above results, we further investigated the feasibility of this sensor for real samples by analyzing the microRNA-21 expression levels in the total small RNAs extracted from a human cancerous cell line, A549. As shown in Fig. 4, the ECL intensity responses of the biosensor to the lysate from the A549 cells indicated that microRNA-21 was overexpressed in those cells. More importantly, there is a certain correlation that the ECL intensity increased as the number of A549 cells increased. This confirms the feasibility of the biosensor for the analysis of real samples, indicating that our proposed strategy has great potential for early diagnosis of cancers.

Conclusion

A novel electrocheminuminescent DNA biosensor is described using GO as an immobilization substrate. The introduction of GO in the construction of the biosensor achieved the effective loading of hairpin DNA, while the hairpin DNA does not need special modification. Not only did the use of HCR prove an effective strategy for amplifying the detection signal, leading to a low detection limit of microRNA-21, but the proposed biosensor also exhibited good selectivity in the A549 cell line detection.

Acknowledgments This work was financially supported by the National Natural Science Foundation of China (No. 21527808, 21475006) and Beijing municipal high level innovative team building program (IDHT 20180504).

Compliance with ethical standards The author(s) declare that they have no competing interests.

References

1. Baffa R, Fassan M, Volinia S, O'Hara B, Liu CG, Palazzo JP, Gardiman M, Rugge M, Gomella LG, Croce CM, Rosenberg A (2009) MicroRNA expression profiling of human metastatic cancers identifies cancer gene targets. J Pathol 219(2):214–221
2. Engels BM, Hutvagner G (2006) Principles and effects of microRNA-mediated post-transcriptional gene regulation. Oncogene 25(46):6163–6169
3. Meister G, Tuschl T (2004) Mechanisms of gene silencing by double-stranded RNA. Nature 431(7006):343–349
4. Valoczi A, Hornyik C, Varga N, Burgyan J, Kauppinen S, Havelda Z (2004) Sensitive and specific detection of microRNAs by northern blot analysis using LNA-modified oligonucleotide probes. Nucleic Acids Res 32(22):e175
5. Yu CY, Yin BC, Ye BC (2013) A universal real-time PCR assay for rapid quantification of microRNAs via the enhancement of base-stacking hybridization. Chem Commun 49(74):8247–8249
6. Lim LP, Lau NC, Garrett-Engele P, Grimson A, Schelter JM, Castle J, Bartel DP, Linsley PS, Johnson JM (2005) Microarray analysis shows that some microRNAs downregulate large numbers of target mRNAs. Nature 433(7027):769–773
7. Lu LP, Liu C, Kang TF, Miao WJ, Wang XY, Guo GS (2018) In situ enhanced electrochemiluminescence based on co-reactant self-generated for sensitive detection of microRNA. Sensors Actuators B (255):35–41
8. Jiang L, Duan DM, Shen Y, Li J (2012) Direct microRNA detection with universal tagged probe and time-resolved fluorescence technology. Biosens Bioelectron 34(1):291–295
9. Fang SP, Lee HJ, Wark AW, Corn RM (2006) Attomole microarray detection of MicroRNAs by nanoparticle-amplified SPR imaging

measurements of surface polyadenylation reactions. J Am Chem Soc 128(43):14044–14046
10. Heydari-Bafrooei E, Askari S (2017) Ultrasensitive aptasensing of lysozyme by exploiting the synergistic effect of gold nanoparticle-modified reduced graphene oxide and MWCNTs in a chitosan matrix. Microchim Acta 184:3405–3413
11. Ensafi AA, Heydari-Bafrooei E, Dinari M, Mallakpour S (2014) Improved immobilization of DNA to graphite surfaces, using amino acid modified clays. J Mater Chem B 2:3022–3028
12. Ensafi AA, Nasr-Esfahani P, Heydari-Bafrooei E, Rezaei B (2014) Redox targeting of DNA anchored to MWCNTs and TiO2 nanoparticles dispersed in poly dialyldimethylammonium chloride and chitosan. Colloids Surf B: Biointerfaces 121:99–105
13. Heydari-Bafrooei E, Shamszadeh NS (2017) Electrochemical bioassay development for ultrasensitive aptasensing of prostate specific antigen. Biosens Bioelectron 91:284–292
14. Zhang R, Chen A, Yu Y, Chai Y, Zhuo Y, Yuan R (2018) Electrochemiluminescent carbon dot-based determination of microRNA-21 by using a hemin/G-wire supramolecular nanostructure as co-reaction accelerator. Microchim Acta 185:432
15. Jian Y, Wang H, Lan F, Liang L, Ren N, Liu H, Ge S, Yu J (2018) Electrochemiluminescence based detection of microRNA by applying an amplification strategy and hg(II)-triggered disassembly of a metal organic frameworks functionalized with ruthenium(II)tris(bipyridine). Microchim Acta 185:133
16. Huang KJ, Liu YJ, Zhang JZ, Cao JT, Liu YM (2015) Aptamer/au nanoparticles/cobalt sulfide nanosheets biosensor for 17 beta-estradiol detection using a guanine-rich complementary DNA sequence for signal amplification. Biosens Bioelectron 67:184–191
17. Zhang P, Wu XY, Chai YQ, Yuan R (2014) An electrochemiluminescent microRNA biosensor based on hybridization chain reaction coupled with hemin as the signal enhancer. Analyst 139(11):2748–2753
18. Erdem A, Muti M, Mese F, Eksin E (2014) Chitosan-ionic liquid modified single-use sensor for electrochemical monitoring of sequence-selective DNA hybridization. Colloids Surf B: Biointerfaces 114:261–268
19. Yang WR, Ratinac KR, Ringer SP, Thordarson P, Gooding JJ, Braet F (2010) Carbon nanomaterials in biosensors: should you use nanotubes or graphene? Angew Chem Int Ed 49(12):2114–2138
20. Shao YY, Wang J, Wu H, Liu J, Aksay IA, Lin YH (2010) Graphene based electrochemical sensors and biosensors: a review. Electroanalysis 22(10):1027–1036
21. Wu M, Kempaiah R, Huang PJJ, Maheshwari V, Liu JW (2011) Adsorption and desorption of DNA on graphene oxide studied by fluorescently labeled oligonucleotides. Langmuir 27(6):2731–2738
22. Huang R, Liao YH, Zhou XM, Xing D (2015) Toehold-mediated nonenzymatic amplification circuit on graphene oxide fluorescence switching platform for sensitive and homogeneous microRNA detection. Anal Chim Acta 888:162–172
23. Agudelo D, Bourassa P, Berube G, Tajmir-Riahi HA (2014) Intercalation of antitumor drug doxorubicin and its analogue by DNA duplex: structural features and biological implications. Int J Biol Macromol 66:144–150
24. Carvalho C, Santos RX, Cardoso S, Correia S, Oliveira PJ, Santos MS, Moreira PI (2009) Doxorubicin: the good, the bad and the ugly effect. Curr Med Chem 16(25):3267–3285
25. Yang XP, Lin J, Liao XL, Zong YY, Gao HH (2015) Interactions between N-acetyl-L-cysteine protected CdTe quantum dots and doxorubicin through spectroscopic method. Mater Res Bull 66:169–175
26. Li CX, Wang HY, Shen J, Tang B (2015) Cyclometalated iridium complex-based label-free Photoelectrochemical biosensor for DNA detection by hybridization chain reaction amplification. Anal Chem 87(8):4283–4291
27. Liu T, Chen X, Hong CY, Xu XP, Yang HH (2014) Label-free and ultrasensitive electrochemiluminescence detection of microRNA based on long-range self-assembled DNA nanostructures. Microchim Acta 181(7–8):731–736
28. Brownson DAC, Munro LJ, Kampouris DK, Banks CE (2011) Electrochemistry of graphene: not such a beneficial electrode material? RSC Adv 1(6):978–988
29. Yan Z, Li Y, Zheng JB, Zhou M (2014) Electrogenerated chemiluminescence biosensing method for methyltransferase activity using tris(1, 10-phenanthroline) ruthenium-assembled graphene oxide. J Electroanal Chem 731:133–138
30. Rafiee-Pour HA, Behpour M, Keshavarz M (2016) A novel label-free electrochemical miRNA biosensor using methylene blue as redox indicator: application to breast cancer biomarker miRNA-21. Biosens Bioelectron 77:202–207
31. Azimzadeh M, Rahaie M, Nasirizadeh N, Ashtari K, Naderi-Manesh H (2016) An electrochemical nanobiosensor for plasma miRNA-155, based on graphene oxide and gold nanorod, for early detection of breast cancer. Biosens Bioelectron 77:99–106
32. Xiong HT, Zheng XW (2017) Electrochemiluminescence based determination of micro-RNA using target-guided assembly of gold nanoparticles on an electrode modified with Nafion, carbon nanotubes and polyvinylpyrrolidone. Microchim Acta 184(6):1781–1789
33. Zhang TT, Zhao HM, Fan GF, Li YX, Li L, Quan X (2016) Electrolytic exfoliation synthesis of boron doped graphene quantum dots: a new luminescent material for electrochemiluminescence detection of oncogene microRNA-20a. Electrochim Acta 190:1150–1158
34. Park KW, Batule BS, Kang KS, Park KS, Park HG (2016) Rapid and ultrasensitive detection of microRNA by target-assisted isothermal exponential amplification coupled with poly (thymine)-templated fluorescent copper nanoparticles. Nanotechnology 27(42):425502
35. Xu FZ, Luo L, Shi H, He XX, Lei YL, Tang JL, He DG, Qiao ZZ, Wang KM (2018) Label-free and sensitive microRNA detection based on a target recycling amplification-integrated superlong poly(thymine)-hosted copper nanoparticle strategy. Anal Chim Acta 1010:54–61